

Adaptive MCS Selection with Dynamic and Fixed Sub-channelling for Frequency-Coherent OFDM Channels

Muayad S. Al-Janabi, Charalampos C. Tsimenidis, *Member, IEEE*, Bayan S. Sharif, *Senior Member, IEEE* and Stéphane Y. Le Goff School of Electrical, Electronics and Computer Engineering
Newcastle University, Merz Court, NE1 7RU, Newcastle upon Tyne, UK

Abstract—This paper presents two strategies for joint adaptive modulation and coding (AMC) techniques. The first strategy is based on the fixed sub-channel (FS)-AMC allocation, which exploits the coherence bandwidth of the wireless channel to divide the transmitted frame into independent sub-channels that correspond to the channel coherence bandwidth as well as selecting the optimal modulation and coding scheme (MCS) for each individually. The second strategy is based on dynamic sub-channel (DS)-AMC allocation, reduces the size of pilot sub-carriers for the stable sub-channel profiles; where the redundant pilots are replaced with additional data sub-carriers, which enhance the total system throughput. These strategies are implemented for orthogonal frequency division multiplexing (OFDM) systems with channel state information (CSI) feedback. Low density parity check (LDPC) codes are utilized for encoding by employing signal-to noise ratio (SNR) dependent coding rates, as well as distinct modulation schemes to achieve adaptivity to time-varying channel conditions. The performance of the proposed system was tested on Rayleigh fading channels that exhibit frequency coherent bands. Numerical results obtained via simulation demonstrate that the throughput and bit error rate (BER) performances of both proposed systems are better than previously suggested approaches. Additionally, there is a significant improvement in the throughput performance of the dynamic sub-channel allocation strategy over the fixed sub-channel allocation method.

Index Terms—Frequency channel coherent, sub-channelling, OFDM, AMC, MCS.

I. INTRODUCTION

Recently, the requirements for achieving high performance in wireless communications systems have increased dramatically. These requirements have focused on the schemes that increase the transmission of data as well as minimizing the BER at the receiver. OFDM for single user and orthogonal frequency division multiple access (OFDMA) for multiuser are examples of such powerful systems. The above two systems have been adopted by many standards including Fixed WiMAX IEEE 802.16 and Mobile WiMAX IEEE 802.16e. They demonstrate high ability to tackle the degradations introduced by multipath channels that cause inter symbol interference (ISI) at low computational complexities. However, the transmitted waveforms of these systems exhibit high peak-to-average power ratio (PAPR) and are sensitive to Doppler shifts, which produce inter carrier interference (ICI) [1]-[8].

OFDM and OFDMA systems are implemented in practice using error correcting schemes, such as convolutional, turbo

and LDPC codes. In this paper, we adopt LDPC codes since they exhibit lower computational complexity. LDPC codes were invented by Gallager in 1963 as a class of linear codes. Their main feature is a sparse generator matrix which comprises a low density of ones. Nowadays, LDPC codes are widely employed in AMC strategies to select suitable modulation and coding rates for OFDM and OFDMA sub-carriers based on returned CSI. The aim is to avoid the additional iterative processing, which is impractical with real-time systems, since LDPC decoding already incorporates iterations inside its decoder [9]-[11].

Most research studies so far have focused on AMC for OFDM systems without any consideration of the frequency coherence of the underlying wireless channel. In [12], AMC for OFDM schemes was presented, which divided the OFDM frame into fixed clusters, with each cluster exhibiting independent modulation and coding schemes according to CSI that was returned from the receiver. In [13] and [14], the implementation of adaptive bit-interleaved coded modulation (BICM) with OFDM was introduced depending on the returned CSI obtained from the estimated BER. However, they considered the OFDM frame as a one part with same MCS for all symbols. In [15], a novel two-step channel prediction technique has been proposed that considered the time-varying nature of a channel over the duration of interest that produced the required CSI to the transmitter to achieve adaptivity.

Reliable transmission of the information stream was ensured by utilising the lowest and fixed MCS levels in [16]. Moreover, this method was also very efficient for a large number of sharing users per transmitted frame. To increase the system performance, two strategies were used; the first strategy enhanced the system throughput by employing the AMC technique to exploit the capacity of the channel; the second strategy adopted the link-layer auto repeat request (LARQ) and hybrid auto repeat request (HARQ) to increase the transmitted packet error rate and to reduce the convolutional code gain in order to detect the error of the received data packet.

In [17], the AMC technique was used in a wideband code division multiple access (WCDMA) downlink to enhance the scheduling performance; at the same time, a fast cell selection (FCS) strategy was adopted. In this work, the Round Robin (RR), the simplified proportional fair (PF), the maximum carrier to interference ratio(C/I), and the conventional PF schemes were investigated and compared as scheduling techniques.

Moreover, the authors tried to maximise the user throughput in a cellular network by proposing an optimal selection of the MCS options. The system was based on the Chase Combining and Incremental Redundancy schemes for the HARQ mechanism. The optimal MCS selection was dependent on the number of transmissions and successful decoding probability in the HARQ operation.

The authors of [18] adopted the SNR-based and buffer-assisted AMC technique strategies of selection to analyse the channel packet transmission and re-transmission system. In this work, the size and status of the transmit buffers have been considered during the design and analysis of the performance, efficiency, and complexity measurements.

The impact for the estimated channel errors in a CDMA system, which used the AMC strategy with multi-codes, was presented in [19]. Moreover, the communication channel was modelled utilising Simple Moving Average (SMA) and Hidden Markov Model (HMM) filters. In [20], a link adaptation algorithm with Packet Error Rate (PER) was presented. The PER performance was predicted for the coded multiple-antenna OFDM system based on the detected error of the channel estimation.

In [21], a comparison of the throughput performance between Single-Carrier transmission with Frequency-Domain Equalisation (SCFDE) and OFDM over the non-linear fading channels was presented. The transmitted power was used as a metric with the AMC criteria to overcome the transmission drawbacks. On the other hand, an efficient Medium Access Control (MAC) technique based on AMC strategy was presented in [22]. The packet format was varied based on the channel state to achieve a high performance system and an optimal analytical model was proposed for the non-stationary transmission link. In addition, a comparison between the analytical evaluations and simulation results was presented to show the outperformance of the proposed system. Additionally, in [23], a cross-layer design over the data link and physical layer was derived, the optimal system performance was achieved by exploiting the truncated ARQ protocol ability to correct the transmission errors as well as the using AMC strategy features.

Issues concerning the distribution methods of the pilot along the OFDM frame have been widely addressed in recent research work. The two main prevailing approaches are the block and comb pilot distribution methods [24]-[26].

The first key contribution of our paper is to produce an FS-AMC-OFDM scheme that exploits the frequency coherence of the channel by dividing the OFDM frame into sub-channels that correspond to the detected channel coherence bands at the receiver. Subsequently, each individual sub-channel is assigned its own independent MCS. The second contribution is to present a DS-AMC-OFDM system, which reduces the number of pilot sub-carriers within the individual stable profile sub-channels and replaces the unused sub-carriers by additional information streams. This reduction is dependent on the SNR fluctuation values of the sub-channels, and the sub-channels' minimum SNR values. Moreover, in order to achieve an optimum channel estimate, pilots are inserted and interleaved across the frame data using the comb method [24]-[25]. The

proposed AMC strategy is established on six adapting options that support the flexibility of switching between MCS schemes in real time to reach the required performance.

The remainder of the paper is organized as follows. In Section II, the description of the proposed system is presented. Section III outlines the LDPC decoding algorithm, while the proposed transmission techniques is introduced in Section IV. Section V demonstrates the performance of the proposed systems via simulation results. Finally, conclusions are drawn in Section VI.

II. SYSTEM MODEL DESCRIPTION

This section outlines the proposed FS-AMC-OFDM and DS-AMC-OFDM systems. In these schemes, LDPC codes are considered with three different coding rates in conjunction with two modulation schemes, i.e. 16 quadrature amplitude modulation (16-QAM) and quadrature phase shift keying (QPSK) modulation. These two modulation types combined with three coding rates produce six individual MCSs.

The transmitted OFDM frame of the proposed system contains N sub-carriers, which are divided into N_p pilots, N_d data, and N_G guard sub-carriers. The pilots are distributed uniformly into groups corresponding to the number of detected frequency coherence bands N_{coh} of the channel.

For the FS-AMC-OFDM system, each sub-channel adopts a distinct MCS and contains $\alpha_d(i) = N_d/N_{\text{coh}}$ data and $\alpha_p(i) = N_p/N_{\text{coh}}$ pilot sub-carriers, where $i = \{1, \dots, N_{\text{coh}}\}$ is the index of the sub-channels. The number of the selected MCS for each group of symbols is sent to the transmitter via the returned CSI, instead of estimating the channel and SNR values in order to reduce the size of the feedback information required. On the other hand, the size of data $\alpha_d(i)$ and pilot $\alpha_p(i)$ sub-carriers, within sub-channels can be changed for DS-AMC-OFDM system according to the returned channel conditions. The CSI is assumed to be returned using time division duplex (TDD) link without any feedback delay due to the short transmission distance.

The proposed systems are applicable in many transmission environments and they require identical implementation complexity to the related conventional AMC based transmission schemes that utilize same MCSs. The proposed systems are described in detail in the following sub-sections.

A. FS-AMC-OFDM system

The investigated FS-AMC-OFDM system can be divided into the following three parts.

1. Transmitter: The transmitter comprises three main blocks as shown in Fig. 1. The first block generates, from the binary data, different coded and modulated symbol groups that are assigned to different sub-channels. The second block assembles the OFDM signalling frame from the modulated data and the pilots, which are inserted at uniform positions using a comb approach. The final part of the transmitter implements the inverse fast Fourier transform (IFFT) and CP

insertion operations. The transmitted OFDM frame can be mathematically represented as:

$$x(k) = \frac{1}{\sqrt{N_{\text{FFT}}}} \sum_{n=1}^{N_{\text{FFT}}} X(n) e^{j \frac{2\pi k n}{N_{\text{FFT}}}}, \quad (1)$$

where $x(k)$ are the transmitted OFDM waveform samples in time-domain, $X(n)$ denotes the OFDM symbols assigned to each data sub-carrier, N_{FFT} is the FFT size and $k = \{1, \dots, N_{\text{FFT}}\}$ and $n = \{1, \dots, N_{\text{FFT}}\}$ are the time and frequency domain indices, respectively.

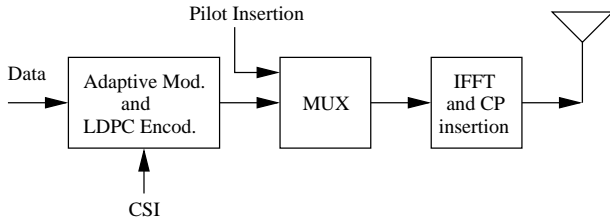


Fig. 1. Transmitter block diagram of the proposed FS-AMC-OFDM system.

2. Channel Model: It is known that there are many types of coherent channels, such as time variant and invariant channels for both fast and slow fading. The frequency response of these channels can be more or less selective in terms of the selected sub-carriers. This selectivity may decrease the coherence bandwidth, which in turn increases the utilized sub-channels in our proposed system.

In this paper, a wireless Rayleigh fading communication channel is considered in this paper. A key assumption is that the channel exhibits coherence frequency bands, thus, the total system bandwidth is divided into sub-channels that are time-varying but flat in terms of attenuation for all sub-carriers within the same band. The individual sub-channel values are assumed to be correlated between subsequent symbols. The impulse response of the channel is given as:

$$h(k) = \sum_{l=0}^{L-1} h_l(k) \delta(\tau_l), \quad (2)$$

where L is the number of taps, τ_l is the time delay associated with the l -th tap and $h_l(k)$ is the complex-valued channel fading coefficient of the l -th tap for the time index k . The coherence bandwidth B_{coh} , which represents the frequency correlation between channel gains, is given for values above 0.9 as:

$$B_{\text{coh}} = \frac{1}{50\sigma_\tau}, \quad (3)$$

where σ_τ is the root mean square (rms) of the multipath delay spread in the time domain, given as:

$$\sigma_\tau = \sqrt{\frac{\sum_{l=0}^{L-1} |h_l(k)|^2 \tau_l}{\sum_{l=0}^{L-1} |h_l(\tau_l)|^2}}. \quad (4)$$

Fig. 2 demonstrates an example of the system channel with 20 MHz bandwidth suited to propagate one OFDM frame. This model is based on the Rayleigh channel properties and exhibits

15 taps. In this figure, part (a) represents the the channel time impulse response, while (b) is the channel frequency response in dB.

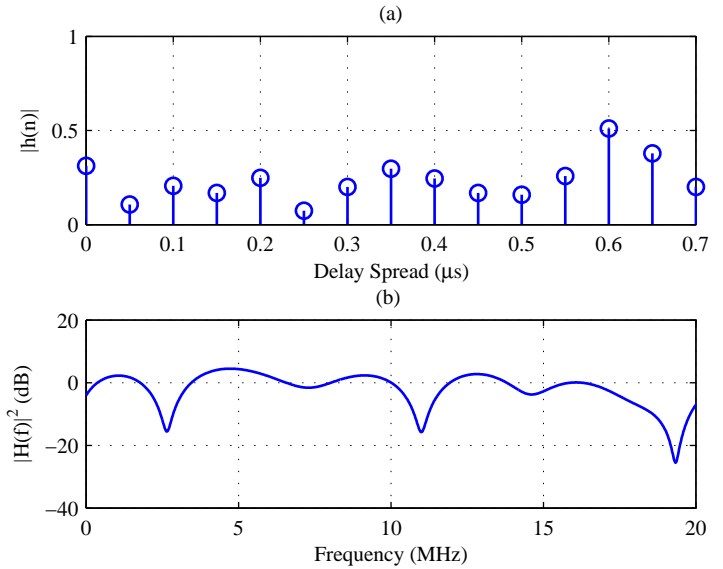


Fig. 2. Channel model.

3. Receiver Description: The receiver structure is illustrated in Fig. 3. After the cyclic prefix has been removed, the received OFDM frame can be represented as:

$$y(k) = r(k) + w(k) = x(k) \otimes h(k) + w(k), \quad (5)$$

where $y(k)$ are the received samples, $h(k)$ refers to the channel coefficients, $w(k)$ represents the additive white Gaussian noise (AWGN) samples, \otimes denotes the circular convolution operation. The result of the circular convolution, $r(k)$, between the transmitted OFDM samples and the channel values is defined as:

$$r(k) = \sum_{l=0}^{L-1} h(l) x((k-l))_N, \quad k = 0, \dots, N-1. \quad (6)$$

After the FFT operation is applied to the entire OFDM frame, the received signal samples can be expressed as:

$$Y(n) = X(n)H(n) + W(n). \quad (7)$$

Following the FFT operation, the pilots and the data are extracted from the received OFDM frame. The pilots are utilized in the channel estimation algorithm and CSI unit, which produces the estimated channel and SNR values, as well as, the decision of suitable MCS for each sub-channel. Finally, the data are demodulated and decoded in the same selected transmitted MCSs. In this paper, a Mobile WiMAX IEEE 802.16e system is considered with the parameters listed in Table I. The performance of the investigated FS-AMC-OFDM system is effected by many utilized parameters, such as the data and pilot sub-carriers number as well as the employed bandwidth.

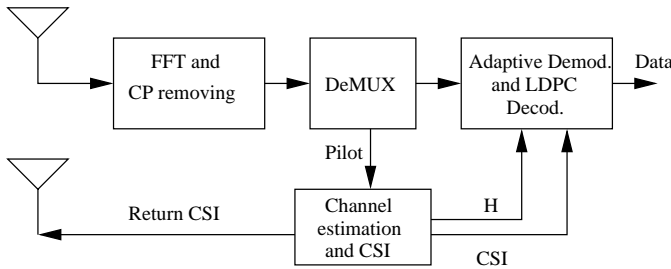


Fig. 3. Receiver block diagram of the proposed FS-AMC-OFDM system.

TABLE I
SYSTEM PARAMETERS

No	Parameter	Value
1	Bandwidth	20 MHz
2	Number of FFT	2048
3	Number of data carrier	1440
4	Number of pilot carrier	240
5	Number of guard sub-carrier	368
6	Cyclic prefix	1/4
7	Coherence bandwidth	4 MHz

B. DS-AMC-OFDM system

This section considers the developments applied to the FS-AMC-OFDM system structure in order to produce an efficient scheme, which uses dynamic allocation for the data and pilot sub-carriers across the distinct sub-channels instead of a fixed allocation strategy. The transmitter block diagram of the proposed DS-AMC-OFDM system is similar to FS-AMC-OFDM, where the first block (Adaptive Mod. and LDPC Encod.) decides the size of the transmitted information bit stream for each sub-channel according to the returned CSI. At the same time, the pilot generator can reduce or increase the pilot stream size for each coherence bands based on the corresponding returned pilot size.

The selectivity of the utilized channel frequency response can effect the performance of the DS-AMC-OFDM system particularly for the narrow coherence bandwidth channels. For these channels, the proposed system uses all the employed pilots for channel estimation. We use the same channel model of the FS-AMC-OFDM system, while the receiver adds another block to adjust the size of the data and pilot symbols for each sub-channel individually as explained in the next section.

1. Reciever: Fig. 4 illustrates the DS-AMC-OFDM system receiver. From this figure, the size of the pilot and data for each sub-channel is adjusted in the additional, Size Adjustment, block. The main function of the new block is to decide a suitable size for the data and pilot across the sub-channels individually, while the other receiver's blocks have the same functions of the FS-AMC-OFDM system receiver. For stable channel conditions, the pilots' size is reduced and the available size from this reduction is filled with additional data symbols at the transmitter to increase the total transmission throughput. The selected sizes of the pilots of each sub-channel is included

in the returned CSI.

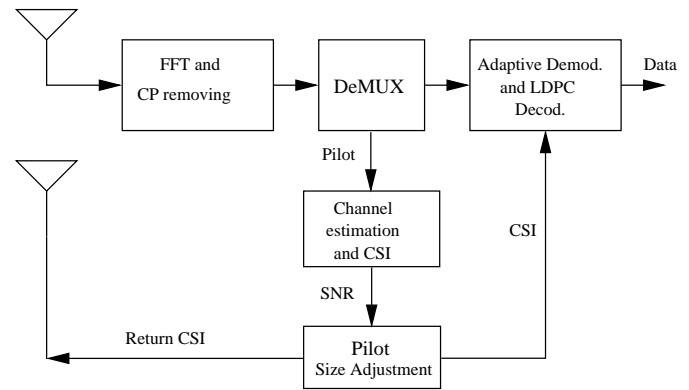


Fig. 4. Receiver block diagram of the proposed DS-AMC-OFDM system.

III. LDPC DECODING

As the proposed systems follow the Mobile WiMAX standard, we employ LDPC as one of the recommended error correction methods. The LDPC codes that have been adopted in this paper are irregular repeat accumulate codes which have a high ability to detect and correct the receiving errors depending on the error probability density function (pdf). The LDPC encoding and decoding processes are explained as follows.

A. LDPC encoder

LDPC encoding is performed by generating a parity check matrix, which must be a sparse matrix with a specified number of columns and rows according to the codeword size and employed code rate respectively. To obtain the encoded data sequence, the entire binary data vector is multiplied by a generator matrix, which is derived from the parity check matrix [27]. Fig. 5 shows the LDPC encoding process block diagram.

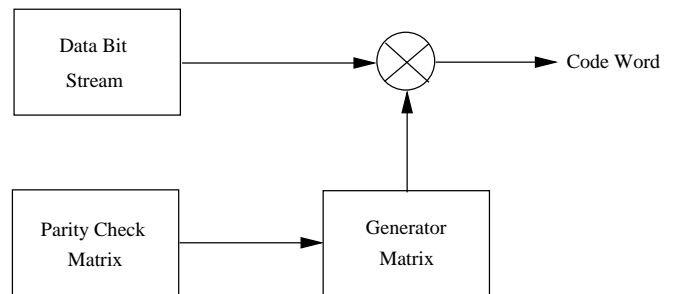


Fig. 5. LDPC encoder block diagram.

B. LDPC decoder

The algorithms performing the LDPC decoding process produce efficient and iterative methods to decode the received data bits. In this paper the message passed algorithm

is adopted. This algorithm is also known as the belief propagation algorithm, and sum-product algorithm. The message passed algorithm is based on decoding the coded bits in iterative manner as a message between the bit and check nodes shown in Fig. 6 illustrating the Tanner graph. It is implemented using four processing steps, i.e. initialization, check node update, bit node update and hard decision. We now proceed with the description of the individual steps [27].

1. *Initialization:* Set the loop iteration, $l = 0$,

$$\eta_{m,n}^{[0]} = 0, \quad \forall (m, n) \text{ with } A(m, n) = 1, \quad (8)$$

$$\lambda_n^{[0]} = L_c r_n. \quad (9)$$

where \mathbf{A} is the parity check matrix, L_c is the channel reliability, λ and η are the messages from bit nodes to check nodes, and check to bit nodes, respectively.

2. *Check node update:*

$$l = l + 1. \quad (10)$$

$$\eta_{m,n}^{[l]} = -2 \tanh^{-1} \left(\prod_{j \in N_{m,n}} \tanh \left(-\frac{\lambda_j^{[l-1]} - \eta_{m,j}^{[l-1]}}{2} \right) \right). \quad (11)$$

3. *Bit node update:*

$$\lambda_n^l = L_c r_n + \sum_{m \in M_n} \eta_{m,n}^{[l]}. \quad (12)$$

4. *Hard decision:*

$$c_n = \begin{cases} 1, & \text{if } \lambda_n > 0 \\ 0, & \text{otherwise} \end{cases} \quad (13)$$

if $(\mathbf{A}\mathbf{c}' = 0)$, then stop;
 else if $(l < L)$ go to check node update;
 otherwise exit;
 Here, c_n are the decoded data bits, L is the maximum number of iterations, and \mathbf{c}' is the vector containing the decoded bits at the end of the final iteration.

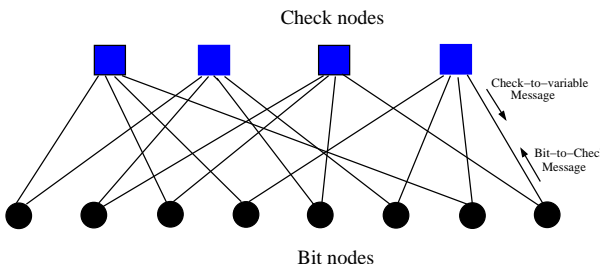


Fig. 6. LDPC decoding algorithm Tanner graph.

IV. PROPOSED AMC-LDPC-OFDM TRANSMISSION TECHNIQUES

The LDPC encoder encodes the entire data sequence using one of the three possible code rates (1/2, 2/3 or 3/4). Furthermore, two modulation schemes are available for sub-channels in order to satisfy their selected MCSs, i.e. QPSK and 16-QAM. In this section, the proposed transmission strategies of both systems are described separately.

A. FS-AMC-OFDM strategy

The novelty of this system is the introduction of distinct MCSs that correspond to the detected frequency coherent sub-channels. The N_p pilots are modulated using BPSK to guarantee insensitivity to channel effects at both low and high SNR levels. Additionally, they are distributed across the data symbols according to the comb-method by allocating one pilot carrier for every six data symbols, as illustrated in Fig. 7.

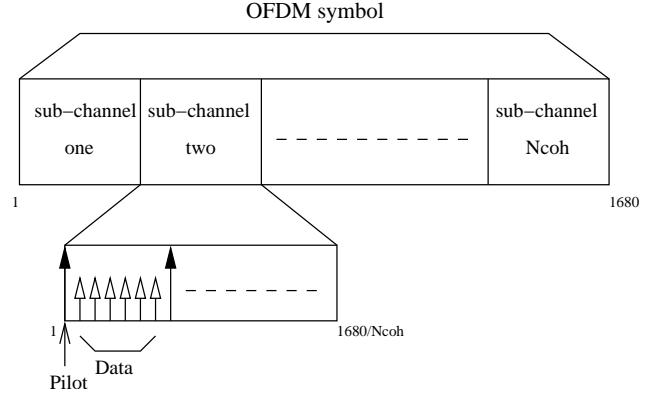


Fig. 7. AMC-LDPC-OFDM transmitted block frame.

At the receiver, channel and SNR estimation, as well as the decision on MCS selection for each sub-channel are performed. The channel estimation was implemented using the least square (LS) method [28]:

$$\hat{H}_p(i, m) = D[X_p(i, m)]^{-1} Y_p(i, m), \quad m = 0 \dots \alpha_p(i) - 1, \quad (14)$$

where $\hat{H}_p(i, m)$ are the estimated pilot channel values, $D[X_p(i, m)]$ is a diagonal matrix constructed using the known transmitted pilot symbols, and $Y_p(i, m)$ are the received pilot symbols after the FFT operation. In this paper, the channel estimation error is not considered. It is caused by imperfect synchronization, feedback delay and channel estimation. The channel estimation error can be added as a noise to the received signal as $Y(n) = X(n)\hat{H}(n) + X(n)[H(n) - \hat{H}(n)] + W(n)$. Furthermore, the channel estimation error effects the computed value of the corresponding SNR, where $\hat{H}(n)$ denotes the estimated channel coefficients. The channel values that relevant to the data sub-carrier are obtained by averaging neighbour pilots instead of using interpolation methods to reduce the complexity. A two-sample average was utilized based on the assumption that the channel will remain constant throughout the duration of an OFDM block, i.e.

$$\hat{H}_d(i, z) = \frac{1}{2} \left[\hat{H}_p(i, m) + \hat{H}_p(i, m + 1) \right], \quad (15)$$

$$m = \text{mod}(z, N_p), \quad z = 0 \dots (\alpha_d(i)/\alpha_p(i)) - 1, \quad (16)$$

where $\hat{H}_d(i, z)$ represents the z -th data sub-carriers between two pilots for each sub-channel, and m denotes the index of corresponding pilot.

Furthermore, the SNR is estimated for each symbol in the OFDM frame and the minimum value for each sub-channel

$\gamma_{i,\min}$ is selected to guarantee that the required performance is maintained:

$$SNR_d(i, v) = \frac{E\{|\hat{H}_d(i, v)|^2 |X(i, v)|^2\}}{E\{|W(i, v)|^2\}} \quad (17)$$

$$= \frac{E\{|\hat{H}_d(i, v)|^2\} E\{|X(i, v)|^2\}}{E\{|W(i, v)|^2\}} \quad (18)$$

$$= E_s \frac{E\{|\hat{H}_d(i, v)|^2\}}{\sigma_W^2(i, v)} \quad (19)$$

where $\sigma_W^2(i, v)$ is the AWGN variance, $E_s = E\{|X(i, v)|^2\}$ is the average sub-channel symbol energy, which is 1 for QPSK and $10d^2$ for 16-QAM, where d is the minimum distance between constellation points. In practice, we can replace $E\{|\hat{H}_d(i, v)|^2\}$ with the estimated channel values $|\hat{H}_d(i, v)|^2$, where $v = \{1, \dots, \alpha_d(i)\}$ is the sub-channel data symbols index. The minimum SNR is then obtained as:

$$\gamma_{i,\min} = \min[SNR_d(i, v)] = \min \left\{ E_s \frac{|\hat{H}_d(i, v)|^2}{\sigma_W^2(i, v)} \right\} \quad (20)$$

The selection of suitable MCS for each sub-channel is based on the estimated SNR of the corresponding sub-channel according to Table II, which considers the threshold SNR values for a BER of 10^{-3} [12]. The diversity of MCSs

TABLE II
SNR THRESHOLD VALUES FOR MCS

Modulation type	Code rate	Threshold dB
QPSK	1/2	4.5
QPSK	2/3	5.6
QPSK	3/4	8.2
16-QAM	1/2	10.5
16-QAM	2/3	11.9
16-QAM	3/4	> 11.9

for symbol groups that are included in the same OFDM frame improves the system throughput μ by increasing the transmitted throughput $\psi_{av}(i)$, which depends on the sub-channel symbol coding rate $R_c(i)$ and the modulation order $M(i)$, and is given as [12]:

$$\psi(i, v) = \log_2[M(i)]R_c(i). \quad (21)$$

In terms of the probability of the MCS selection, the system throughput can be mathematically expressed as:

$$\mu = \sum_{i=1}^{N_{MCS}} P_r\{MCS(i)\} \psi_{av}(i) (1 - SER), \quad (22)$$

where $P_r\{MCS(i)\}$ denotes the probability of choosing each MCS, $\psi_{av}(i) = E\{\psi(i, n)\}$ is the average transmitted throughput in bit/symbol, SER is symbol error rate and N_{MCS} is the number of MCSs. Additionally, the decrease of SER , which depends on selection of the optimum MCS for the channel type ($P_r\{MCS(i)\}$), leads to an increase in the system throughput as shown in Eq. (22).

On the other hand, the system throughput can be expressed in terms of the size of the transmitted data of each sub-channel, $\alpha_d(i)$, the average transmitted throughput, $\psi_{av}(i)$, and the average sub-channel bit error rate, $P_e(i)$, as follows:

$$\mu = \sum_{i=1}^{N_{coh}} \alpha_d(i) \psi_{av}(i) [1 - P_e(i)]. \quad (23)$$

From Eq. (23), the throughput, which is the successful received bits, is based mainly on the size of the transmitted data symbols. This leads to the ability of enhancing the proposed system throughput performance by increasing the transmitted data size as explained in the next section.

B. DS-AMC-OFDM strategy

The proposed DS-AMC-OFDM system exploits the scalability of OFDM systems such as Mobile WiMAX, which endorses the reduction in pilots, to improve the throughput by replacing the unnecessary pilots within a channel coherence band with information data streams; and hence increase the total transmitted throughput. This reduction in the number of pilots for each sub-channel individually depends on the variance of the sub-channel SNR fluctuation values, $\Gamma_{var}(i)$, and the sub-channel $\gamma_{i,\min}$. The range of the pilot reduction $\lambda(i)$ can be varied between zero and $\alpha_p - 2$.

To measure the coherence bandwidth, which is required to obtain the number of the sub-channels, a correlation process between the channel coefficients is adopted in the frequency domain. It assumes that the correlation between the channel coefficients frequency response depends only on the B_{coh} . The correlation value of the channel can be achieved as:

$$\beta_{B_{coh}} = \frac{E\{[\hat{H}(f) - \eta_{\hat{H}(f)}][\hat{H}(f)(f + B_{coh}) - \eta_{\hat{H}(f+B_{coh})}]^*\}}{E\{|\hat{H}(f)|^2\}} \quad (24)$$

where, $\eta_{\hat{H}(f)}$ and $\eta_{\hat{H}(f+B_{coh})}$ are the mean values of the channel frequency responses, and f is the frequency index. The uniform distribution of the phase of the Rayleigh channels leads to $\eta_{\hat{H}(f)}$ and $\eta_{\hat{H}(f+B_{coh})}$ values to be zero, thus Eq. (24) can be rewritten as:

$$\begin{aligned} \beta_{B_{coh}} &= \frac{E\{[\hat{H}(f)][\hat{H}(f)(f + B_{coh})]^*\}}{E\{|\hat{H}(f)|^2\}} \\ &= \frac{E\{[\hat{H}(f)][\hat{H}(f)(f + B_{coh})]^*\}}{\sigma_{\hat{H}(f)}^2}, \end{aligned} \quad (25)$$

where $\sigma_{\hat{H}(f)}^2$ is the channel variance. By varying the B_{coh} , which is the correlation lag, in an iterative method and keeping the correlation value over 0.9, we can obtain the coherence bandwidth, where the channel responses for frequencies separated by B_{coh} or less, are nearly equal. As a result, N_{coh} is calculated based on the total system bandwidth (BW) as $N_{coh} = \frac{BW}{B_{coh}}$.

The SNR fluctuation of the channel coefficients within each coherence band is evaluated depending on the estimated SNR values as:

$$\Gamma(i, n) = SNR_d(i, v) - \varrho(i), \quad (26)$$

where $\varrho(i) = E\{SNR(i, v)\}$ is the average SNR value for each sub-channel. The $\Gamma_{var}(i)$ value can be calculated as:

$$\Gamma_{var}(i) = E\{|\Gamma(i, n)|^2\}. \quad (27)$$

Based on the detected coherence bandwidth, the number of pilots and data for each sub-channel is set. Moreover, the number of required pilots for the channel estimation is mainly dependent on the fluctuation values between the neighbouring pilots. The SNR values of each sub-channel $\gamma_{i,min}$ are further used to measure the stability of the channel state in terms of the noise. The equations describing the dynamic adjustment of pilots and data streams can be written as:

$$\vartheta_p(i) = \alpha_p(i) - \lambda(i), \quad (28)$$

$$\vartheta_d(i) = \alpha_d(i) - \lambda(i), \quad (29)$$

$$\lambda(i) = \xi(i) \frac{\gamma_{i,min}}{\Gamma_{var}(i)}, \quad (30)$$

where $\vartheta_p(i)$ and $\vartheta_d(i)$ designate the new number of pilots and data for each sub-channel, respectively, and $\xi(i)$ is a variable chosen to satisfy the condition, $\text{mod}[\vartheta_d(i)/\vartheta_p(i)] = 0$, that guarantees a uniform distribution of pilots and data within each sub-channel. The size of the pilot subcarriers of each sub-channel is included in the CSI to permit the transmitter to adjust the transmission sizes. The resulting system throughput, μ , in Eq. (23) can be mathematically rewritten as:

$$\mu = \sum_{i=1}^{N_{coh}} \vartheta_d(i) \rho_{av}(i) [1 - P_e(i)]. \quad (31)$$

Evidently, the increase in the transmitted data stream size is expected to increase the system throughput performance. At the same time, the optimal selection of the suitable MCS for the sub-channels can decrease the BER, which leads to increase the throughput. To measure the effect of the pilot reduction on the channel estimation process, the mean square error (MSE) of the estimated channel value in comparison with the perfect channel $H(i, n)$ and is calculated as:

$$MSE(i) = E\{|\hat{H}(i, n) - H(i, n)|^2\} \quad (32)$$

and the total MSE is evaluated as $TMSE = E\{MSE(i)\}$.

V. SIMULATION RESULTS

The performance of the proposed FS-AMC-OFDM and DS-AMC-OFDM systems are investigated in Rayleigh fading channels exhibiting five frequency coherence bands. The parameters of the Mobile WiMAX standard listed in Table I have been utilized for the simulation. The performance of the investigated systems depends on the utilized parameters for each transmitted OFDM frame. However, both systems still outperform the conventional scheme for the same considered parameters as shown in the next sub-sections. The simulation results of the proposed systems are divided into two parts as follows.

A. FS-AMC-OFDM system

This section demonstrates and discusses the simulation performance of FS-AMC-OFDM system. Fig. 8 shows the throughput comparison between two systems; a conventional adaptive system which adopts the same MCS for the whole OFDM frame, and the proposed adaptive system. It is observed that the proposed scheme provides a throughput related performance gain between 0.1-1.2 Mbit over the conventional adaptive system for a SNR range between 5 and 35 dB. The enhancement in performance is due to the fact that the proposed strategy exploits the channel conditions to construct the transmitted OFDM frame, which contains different types of modulation and coding rates that are related to the coherence bandwidth of the underlying channel. Moreover, the suggested approach benefits from the fading diversity on sub-channels to increase the transmitted throughput, which in turn improves system performance by increasing the coding rate and modulation level as indicated in Eq. (21) and (22). It is worth observing that at high SNR levels above 35 dB the performance of the adaptive systems approximately converges to the same value because they select the same MCS for all sub-channels.

Fig. 9 demonstrates the difference in transmitted throughput between the conventional adaptive and proposed approaches. It is apparent that the performance of proposed system achieves 0.1-0.6 bit/symbol better than the conventional over a SNR range between 5 and 35 dB.

Fig. 10 illustrates the average BER performance as a function of the SNR for the two investigated systems. After 10 dB of SNR, the plot shows clearly the performance advantage of the proposed adaptive scheme. The improvement is due to the optimal MCS selection for each sub-channel, which in turn, enhances the BER performance. However, for high SNR values, the difference in performance between the two adaptive schemes is approximately the same, since their constructed transmitted OFDM frames become nearly identical.

Fig. 11 displays the behaviour of the proposed AMC-LDPC based OFDM system in terms of selecting the maximum reliable data size, which is computed by averaging each

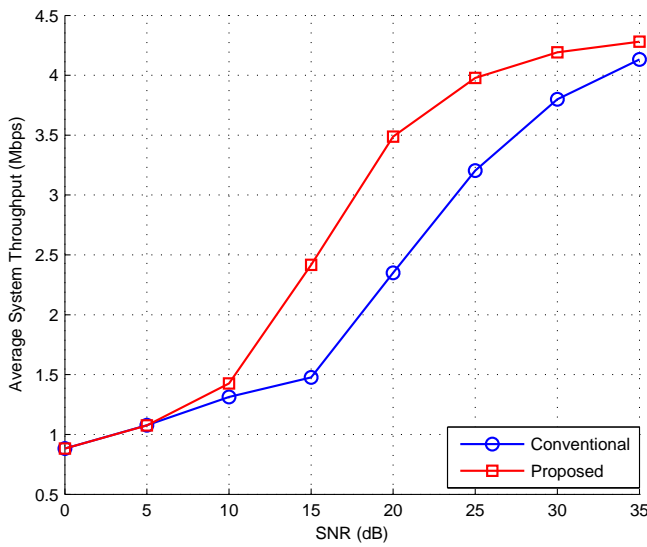


Fig. 8. Throughput of the conventional and proposed FS-AMC-OFDM system.

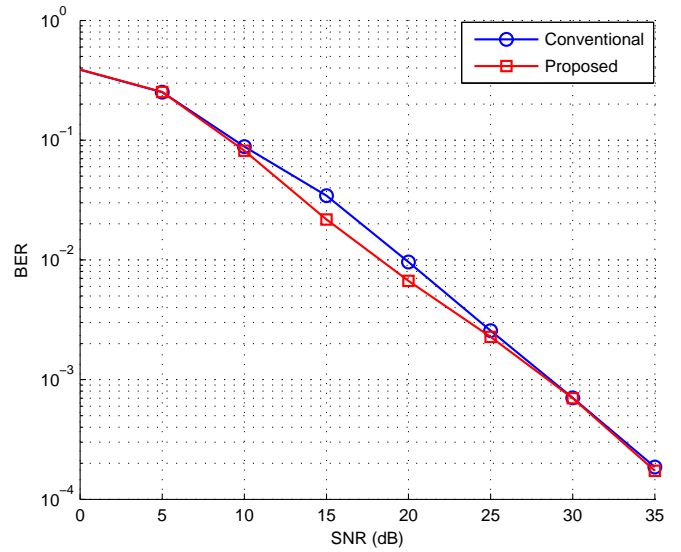


Fig. 10. BER of the conventional and proposed FS-AMC-OFDM system.

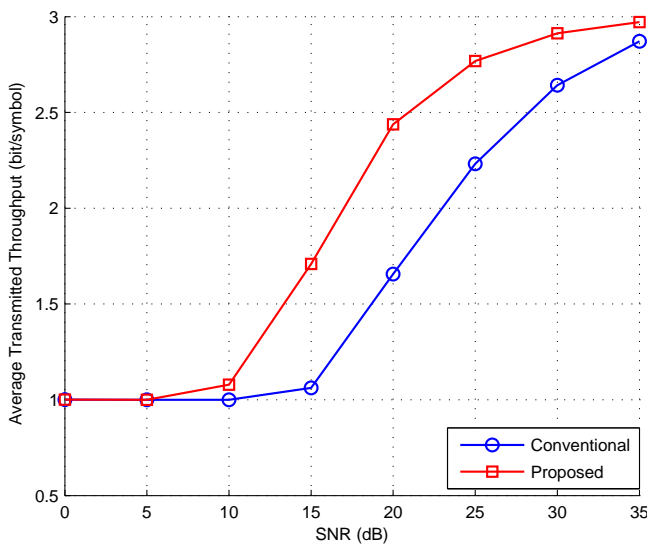


Fig. 9. Transmitted throughput of the conventional and proposed FS-AMC-OFDM system.

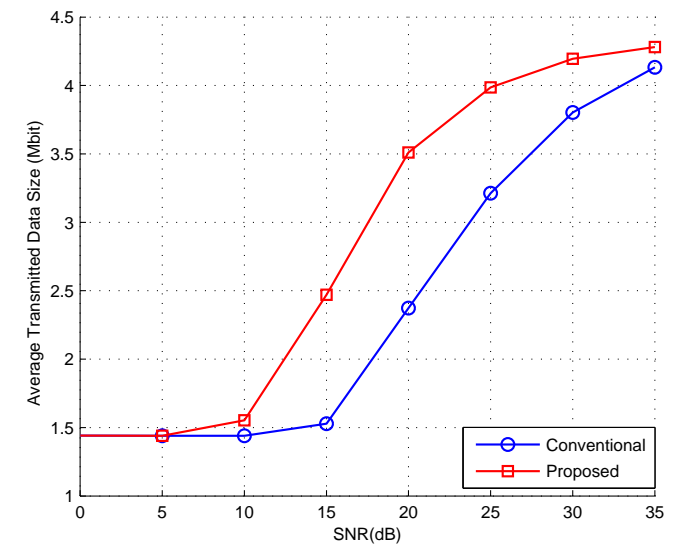


Fig. 11. Transmitted data size of the conventional and proposed FS-AMC-OFDM system.

sub-channel. It should be highlighted that individual points in this graph may contain different types of coding rates and modulation levels. From the diagram, it is apparent that the proposed scheme outperforms the conventional adaptive system. Moreover, it should be noted that at 35 dB of SNR, the data size is chosen to be maximum, indicating that all sub-channels have same modulation type (16-QAM) and coding rate ($R=3/4$).

B. DS-AMC-OFDM system

The simulation results related to the performance of the DS-AMC-OFDM system are presented in this section. The

size of the pilot and data sub-carriers for each sub-channel are adjusted the distinct criteria listed in Table III.

Fig. 12 demonstrates the throughput performance of the conventional, the proposed FS-AMC-OFDM, and the proposed DS-AMC-OFDM systems. It is important to notice that the throughput of proposed DS-AMC-OFDM system outperforms the FS-AMC-OFDM scheme by 0.1-0.7 Mbps over an SNR range of between 5 and 35 dB. At the same time, the investigated DS-AMC-OFDM system can achieve 0.1-1.7 Mbps gains over the conventional adaptive transmission system across the same SNR range. The enhancement of the proposed dynamic sub-channel allocation strategy over the fixed strategy is due mainly to the increase in the transmitted data size according to Eq.

TABLE III
DYNAMIC NUMBER OF THE PILOT AND DATA SYMBOLS FOR EACH SUB-CHANNEL.

$\vartheta_p(i)$	$\vartheta_d(i)$	$\lambda(i)$	$\Gamma_{var}(i)$	$\gamma_{i,\min}(i)$ dB
48	288	0	otherwise	
28	308	20	$0.5 \geq \Gamma_{var}(i) > 0.3$	$10 \leq \gamma_{i,\min}(i) < 20$
8	328	40	$0.3 \geq \Gamma_{var}(i) > 0.2$	$20 \leq \gamma_{i,\min}(i) < 25$
4	332	44	$0.2 \geq \Gamma_{var}(i) > 0.1$	$25 \leq \gamma_{i,\min}(i) < 30$
2	334	46	$\Gamma_{var}(i) \leq 0.1$	$\gamma_{i,\min}(i) \geq 30$

(31). The pilots number is reduced for the stable sub-channel profiles individually, followed by replacing the unused pilot symbols with additional data symbols based on Eq. (28)-(30). On the other hand, the DS-AMC-OFDM scheme throughput improvement in comparison with the conventional AMC method is achieved by the optimal MCS selection for each sub-channel as explained in the previous section. It is observed from the plots that the pilots number reduction has not influenced the performance of the system significantly.

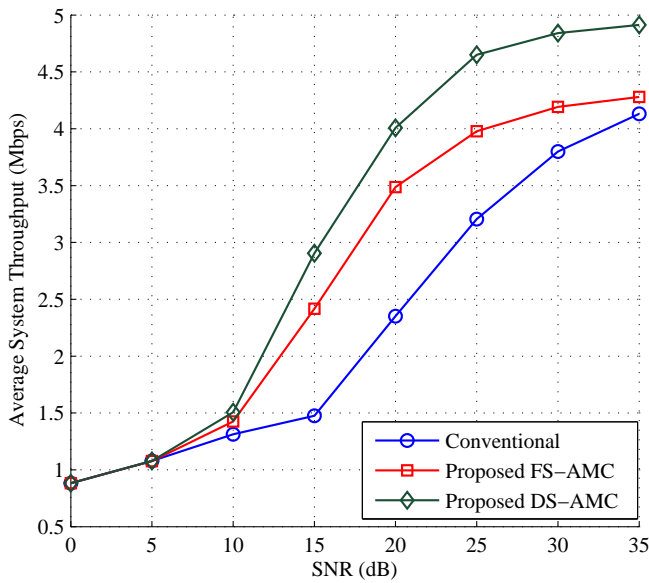


Fig. 12. Throughput of the proposed conventional, FS-AMC-OFDM, and DS-AMC-OFDM systems.

Fig. 13 illustrates the BER performance of the investigated systems. It can be seen that the BER plot for the DS-AMC-OFDM system is approximately converging to the FS-AMC-OFDM scheme. Although there is an increase in the transmitted data size of the DS-AMC-OFDM system, the BER performance is similar to the FS-AMC-OFDM system. It is highlighted that the performance similarity proves that the reduction in pilot size across the sub-channel has not influenced the data recovery, which is based on the channel estimation, at the receiver. Both proposed strategies perform better than the conventional adaptive transmission method, particularly between SNR values of 10 to 25 dB. Meanwhile all compared systems' plots are converging together for high

SNR values due to the similarity of selection the highest MCS for all sub-channels. The BER enhancement of both proposed systems is due to the independent selection of suitable MCS for each sub-channel independently.

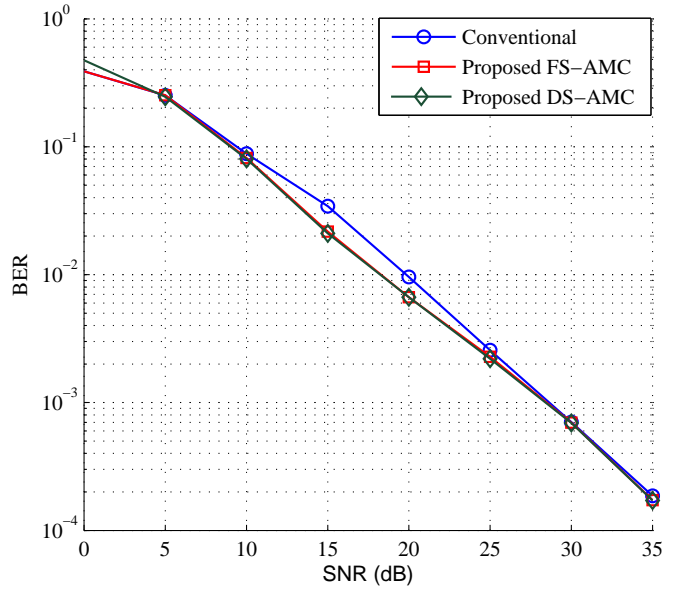


Fig. 13. BER of the conventional, FS-AMC-OFDM, and DS-AMC-OFDM systems.

The comparison of the transmitted data size in bits between the conventional AMC, proposed FS-AMC-OFDM, and proposed DS-AMC-OFDM schemes is presented in Fig. 14. It is observed that the size of the transmitted data for the proposed system based on the dynamic sub-channel allocation strategy is significantly larger by 0.1-0.7 Mbit in comparison with the FS-AMC-OFDM system. Moreover, the DS-AMC-OFDM scheme outperforms the conventional AMC in terms of transmitted data size by 0.1-1.7 Mbit over the SNR range between 5 and 35 dB. The increase in the transmitted data size of the DS-AMC-OFDM system over the other investigated systems is achieved by reducing the number of pilots without affecting the channel estimation performance. Meanwhile, the redundant pilots are replaced by additional data symbols for each sub-channel individually. As mentioned earlier, the reduction in pilot number is restricted by two main metrics; the sub-channel minimum SNR value, and the variance of the sub-channel SNR fluctuation values as expressed in Eq. (30).

In order to monitor the effects of pilot number reduction for each sub-channel independently, the MSE for the estimated channel is evaluated as shown in Fig. 15. The figure shows that the reduction in the number of pilots for the sub-channels with stable profile affects the estimation accuracy after 10 dB. However, the degradation in terms of data recovery errors is acceptable as demonstrated in Fig. 12 in the system throughput performance. The MSE values for both the proposed systems channel estimation is calculated according to Eq. (29).

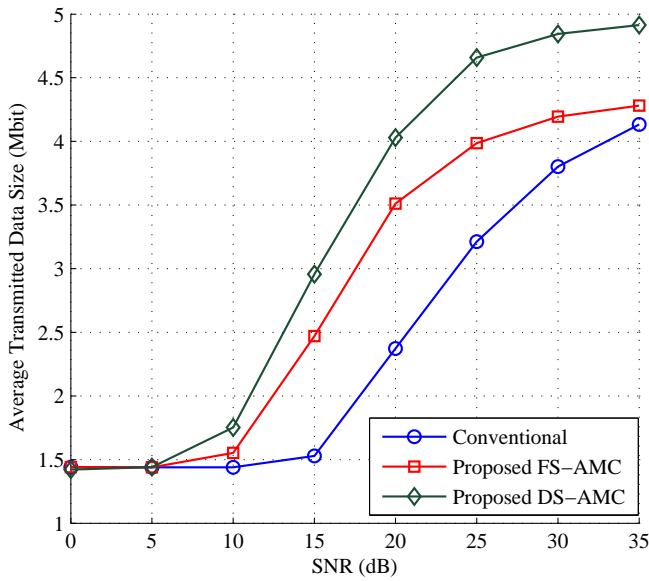


Fig. 14. Transmitted data of the conventional, FS-AMC-OFDM and DS-AMC-OFDM systems.

As a result, the proposed FS-AMC-OFDM and DS-AMC-OFDM systems outperform the conventional approach for different values of SNR. The proposed FS-AMC-OFDM system can perform similar to the conventional scheme over flat fading channels due to the same selection of the MCS level for all sub-channels.

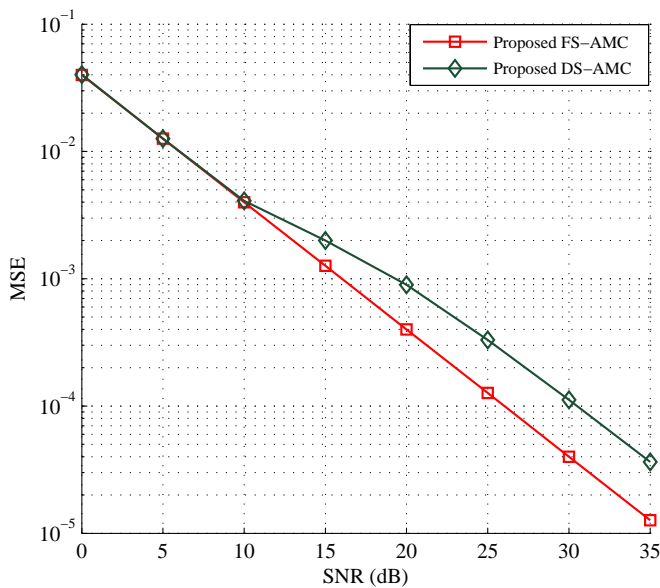


Fig. 15. MSE of the estimated channel for the FS-AMC-OFDM, and DS-AMC-OFDM systems.

VI. CONCLUSIONS

In this paper, we have proposed FS-AMC-OFDM and DS-AMC-OFDM schemes and their performance has been investigated in Rayleigh fading channels. In order to improve the throughput and BER performance of the proposed FS-AMC-OFDM scheme, the detected coherence bandwidth of the channel has been employed as an important indicator for dividing the OFDM frame into distinct sub-channels and subsequently assigning individual modulation schemes and coding rates suited to the corresponding channel conditions. The throughput is improved in the FS-AMC-OFDM system by exploiting the fading diversity of the channel, which results in increased coding rate and modulation orders, which are utilized for sub-channels with stable fading profiles. Moreover, the optimal MCS selection for each sub-channel increases the aggregate system throughput by decreasing the BER due to the optimal utilization of the channel state for each sub-channel at the transmitter.

On the other hand, the throughput performance of the investigated DS-AMC-OFDM system is improved in comparison with the conventional and FS-AMC-OFDM schemes due to the increase in the transmitted data size, achieved by replacing the redundant pilots with data symbols. The redundant pilots result from the pilot reduction across the stable sub-channel profiles, based on the individual sub-channel minimum SNR value, and the variance of the sub-channel fluctuation values. In order to measure the effects of the pilot reduction on the channel estimation process, the MSE value of the estimated channel was evaluated.

Simulation results have demonstrated that both the system throughput and BER of the DS-AMC-OFDM system are improved compared to the FS-AMC-OFDM scheme and conventional adaptive approach. At the same time, the proposed FS-AMC-OFDM scheme also outperforms the conventional system.

Future work will be focused on enhancing the channel estimation methods to further improve in the BER and throughput performances of the proposed strategies. Moreover, it is worth to investigate the ability of implementing the proposed techniques for long term evolution 3rd generation (LTE-3G) systems and discrete multi-tone modulation (DMT) transmission strategies used in digital subscriber lines (DSL), and the implementation restrictions in terms of the utilized system parameters.

REFERENCES

- [1] M. Al-Janabi, C. Tsimenidis, B. Sharif and S. Le Goff, "Adaptive MCS Selection in OFDM Systems Based on Channel Frequency Coherence, *AICT 2009*, pp: 177-182.
- [2] D. Tse, *Fundamentals of Wireless Communications*, University of California, Berkeley, 2004.
- [3] R. van Nee and R. Prasad, *OFDM for Wireless Multimedia Communications*, Artech House, 2000.
- [4] A. L. Intini, *Orthogonal Frequency Division Multiplexing for Wireless Networks*, University of California Santa Barbara, 2000.
- [5] H. Schulze and Ch. Luders, *Theory and Applications of OFDM and CDMA Wideband Wireless Communications*, John Wiley and Sons Ltd, Chichester, 2005.
- [6] U. Madhow, *Fundamentals of Digital Communication*, Cambridge University Press, 2004.

- [7] L. Nuaymi, *WiMAX Technology for Broadband Wireless Access*, John Wiley and Sons, Ltd, England, 2007.
- [8] T. Onodera, T. Nogami, O. Nakamura and N. Okamoto, "AMC Design for Wideband OFDM Maintaining Target Quality Over Time-Varying Channels," *IEEE 18th International PIMRC 2007*, pp:1-5.
- [9] R. G. Gallager, *Low-Density Parity-Check Codes*, MIT Press, Cambridge, MA, 1963.
- [10] D. J. C. MacKay, "Good Error-Correction Codes Based on Very Sparse Matrices", *IEEE Trans. on Inform. Theory*, vol. 45, no. 2, pp: 399-431, Mar. 1999.
- [11] M. Zhou, L. Li, N. Wen, et al., "Performance of LDPC coded AOFDM under frequency-selective fading channel," Intern. Conf. on Commun., *ICCCAS 2006*, pp: 861-865.
- [12] L. Lihua, Z. Mingyu, W. Haifeng and Z. Ping, "LDPC coded AMC based on decoding iteration times for OFDM systems," *VTC 2006*, pp: 1157-1161.
- [13] K. Song, A. Ekbal, S. Chung and J. Cioffi, "Adaptive Modulation and Coding (AMC) for Bit-Interleaved Coded OFDM (BICM-OFDM)", *IEEE Trans. on Wireless Commun.*, vol.5, No.7, pp: 1685-1694, Jul. 2006.
- [14] S. Chung, C. Sung, J. Heo and I. Lee, "Adaptive Bit-Interleaved Coded OFDM With Reduced Feedback Information", *IEEE Trans. Commun.*, Vol.55, No.9, pp: 1649-1655, Sep. 2007.
- [15] J. Heo, Y. Wang, and K. Chang, "A Novel Two-Step Channel-Prediction Technique for Supporting Adaptive Transmission in OFDM/FDD System," *IEEE Trans. Veh. Technol.*, Vol. 57, No. 1, pp: 188-193, Jan. 2008.
- [16] T. Kwon and D. Cho, "Adaptive-Modulation-and-Coding-Based Transmission of Control Message for Resource Allocation in Mobile Communication Systems," *IEEE Trans. Veh. Technol.*, Vol. 58, No. 6, pp: 2769-2782, Jul. 2009.
- [17] H. Fu and D. Kim, "Scheduling Performance in Downlink WCDMA Networks with AMC and Fast Cell Selection," *IEEE Trans. Wireless Commun.*, Vol. 7, No. 7, pp: 2580-2591, Jul. 2008.
- [18] H. Yang and S. Sasakan, "Analysis of Channel-Adaptive Packet Transmission Over Fading Channels With Transmit Management," *IEEE Trans. Veh. Technol.*, Vol. 57, No. 1, pp: 404-413, Jan. 2008.
- [19] R. Kwan and C. Leung, "Performance of a CDMA System Employing AMC and Multicodes in the Presence of Channel Estimation Errors," *IEEE Trans. Commun.*, Vol. 56, No. 2, pp: 189-193, Feb. 2008.
- [20] P. Tan, Y. Wu and S. Sun, "Link Adaptation Based on Adaptive Modulation and Coding for Multiple-Antenna OFDM System," *IEEE J. in Select. Area Commun.*, Vol. 26, No. 8, pp: 1599-1606, Jul. 2008.
- [21] K. Ishihara, Y. Takatori, S. Kubota and M. Umehira, "Comparison of SCFDE and OFDM with adaptive modulation and coding in nonlinear fading channel," *Electronic Letters*, Vol. 43, No. 3, pp: 174-175, Feb. 2007.
- [22] L. Caponi, F. Chiti and R. Fantacci, "Performance Evaluation of a Link Adaptation Technique for High Speed Wireless Communication Systems," *IEEE Trans. Wireless Commun.*, Vol. 6, No. 12, pp: 4568-4575, Dec. 2007.
- [23] X. Wang, Q. Liu and G. Giannakis, "Analyzing and Optimizing Adaptive Modulation Coding Jointly With ARQ for QoS-Guaranteed Traffic," *IEEE Trans. Wireless Commun.*, Vol. 7, No. 7, pp: 1008-1013, Jul. 2008.
- [24] L. Ye, A. Burr, "Adaptive modulation and code rate for turbo coded OFDM transmissions," *VTC 2007*, pp: 2702-2706.
- [25] N. Miki, Y. Kishiyama, M. Sawahashi, "Optimum Adaptive Modulation and Coding Scheme for Frequency Domain Channel-Dependent Scheduling in OFDM Based Evolved UTRA Downlink," *IEEE WCNC 2007*, pp: 1783-1788.
- [26] N. Benvenuto and F. Tosato, "On the Selection of Adaptive Modulation and Coding Modes over OFDM," *Communications, IEEE ICC 2004*, pp: 3251-3255.
- [27] T. Moon, *Error Correction Coding, Mathematical Methods and Algorithms*, John Wiley and sons, INC., Canada, 2005.
- [28] C. Lim and D. Han, "Robust LS Channel Estimation with Phase Rotation for Single Frequency Network in OFDM," *IEEE Transactions on Consumer Electronics* Vol. 52, No. 4, pp: 1173-1178, Nov. 2006.